Virchows Arch [Pathol Anat] (1985) 407:449–456

*Virchows Archiv A*


# Bone marrow lambda-type light chain crystalline structures associated with multiple myeloma

**H. Schvartz [1], P. Bonhomme [2], S. Caulet [1], A. Beorchia [2], M. Patey [1] and T. Caulet [1]**

[1] Laboratoire d'Anatomie Pathologique, Université de Reims – 51, rue Cognacq Jay, F-51100 Reims

[2] Laboratoire de Microscopie Electronique Université de Reims – B.P. 347, F-51062 Reims

**Summary.** A 58-year-old man showed bone marrow crystalline structures associated with a lambda light chain producing multiple myeloma. Analysis and processing of electron images clearly displayed the periodic structure of the crystals. Immunochemistry suggested that they contained the whole or a fragmented constant portion of immunoglobulin.

**Key words:** Multiple myeloma – Crystalline deposits – Ultrastructure – Image analysis

## Introduction

Localized or systemic crystalline cytoplasmic inclusions or deposits associated with plasma cell dyscrasias are rarely reported.

In this paper, we describe the case of a patient who presented with multiple myeloma and unusual lambda light chain crystalline structures in a bone marrow biopsy. We report the histological and ultrastructural features of this biopsy, which was taken before therapy.

## Clinical presentation

A 58-year-old Caucasian male was referred to the hospital in October 1982 because of recent asthaenia, pallor, polyneuritis and bone pains. He had been intermittently treated with non-steroid anti-inflammatory drugs for 20 years for HLA B 27 negative ankylosing spondylitis.

On admission, physical examination was otherwise unremarkable. X rays films of the skeleton demonstrated disseminated punched-out lesions. Erythrocyte sedimentation rate was accelerated, anaemia was marked and the white cell count was reduced. However, the platelet count was normal. Urine immunoelectrophoresis showed a monoclonal lambda light chain spike but the serum electrophoresis was normal. Other clinical laboratory tests were as follows: serum creatinine 167 μmol/l, Ca2+ 2.97 μmol/l, and urinary proteins 2.4 g/D. No significant increase of plasmocytoid cells was found in smears of the bone marrow aspiration. Multiple myeloma diagnosis was confirmed by bone marrow biopsy. Chemotherapy was instituted. The patient is still alive after 2 years.

*Offprint requests to:* H. Schvartz at the above address

## Methods

*Light microscopy*. Bone marrow was fixed in mercuric Holland's fixative for 24 h, decalcified in R.D.O. (Eurobio Co.) for 1 h, dehydrated with ethanol, cleared in xylene, and embedded in paraffin. Sections were cut at 5 μm, deparaffinized with xylene and stained with Haematoxylin and eosin, PAS, Masson trichrome, HPTM, Giemsa, Gordon-Sweet, Congo red and Thioflavine T.

*Immunohistochemistry*. For detection of immunoglobulins Sternberger's unlabeled antibody method of peroxidase antiperoxidase (PAP) was applied to tissue sections.

Using this method, sections were deparaffinized in xylene, washed with 95% alcohol and then with 0.3% hydrogene peroxide in absolute methanol for 30 min. The slides were then rinsed in ethanol. Following three washes with PBS they were incubated with 10% normal goat serum for 30 min, then with one of the following rabbit anti-human primary antisera (Dako Co.) for 90 min each: IgG (1/100), IgM (1/200), IgA (1/800), Kappa (1/1 600), Lambda (1/1 600). The sections were then washed again three times with PBS and incubated with goat anti-rabbit IgG (Dako Co., 1:20) at 37° C for 30 min. After a brief wash in buffer they were incubated with rabbit PAP complex (Dako Co., 1:100) at 37° C for 30 min. After a last wash in PBS for 5 min, the peroxidase was visualized by developing in 3,3′-diaminobenzidine (Serva Co.) and counterstained with haematoxylin. The specificity of the immunoreaction was verified by replacing primary antisera with normal rabbit sera.

*Transmission electron microscopy*. Another sample of bone marrow biopsy was fixed overnight in 2.5% glutaradehyde 0.1 M sodium Cacodylate buffer at pH 7.4 at 4° C, rinsed in 0.1 M sodium Cacodylate at pH 7.4, and post fixed in 2% osmium tetroxide in the same buffer for 1 hour at 4° C. Tissue was dehydrated in ethanol to propylene oxide, and embedded in epoxy resin (Epon). Unstained and stained ultrathin sections with uranyl acetate and lead citrate were prepared and were observed in a 100 kV electron microscope (JEM 100 C). Usually micrographs of each specimen have been recorded with defocus varying by 0.05 μm step from 0 to 0.5 μm. These large focal series allow to optimize the electron microscope contrast transfer function on each observed specimen (phase contrast transfer function for unstained ultrathin sections and amplitude transfer function for stained sections) (Hanszen K.J. – 1971). Magnifications used varied from 10,000 to 200,000.

*Image analysis and processing*. By optical diffractometry of micrographs (Klug A. et al. 1964) the image transfer parameters of the electron microscope were checked (defocus, astigmatism, transferred spatial periods) and image periodicities which were not directly apparent in the image were investigated. When periodicities were discerned (Fig. 3b), optical image processing was employed (Klug A. et al. 1966). Suitable masks (Fig. 3c, d) were placed in the diffraction plane of the diffractometer so that the noise was suppressed in the reconstructed image.

The optical diffractometer (Harburn G. et al. 1972) used a 1 mW Helium Neon laser source and 2 meter focal length transform lenses.

## Results

### *Light microscopy*

All the marrow spaces are devoid of adipocytes and normal haematopoietic cells. They contain numerous square, rectangular or lozenge shaped sharply outlined structures of variable size (50 to 150 μ of length) (Fig. 1a). These structures, gathered in the center of the spaces are homogenous or more frequently stratified and composed of glassy eosinophilic material. Between them plasma cells and some multinucleated giant cells are seen (Fig. 1b). At the periphery of the spaces plasma cell infiltration is seen. No osteoclastic resorption but some crystalline structures are observed in trabecular bone.

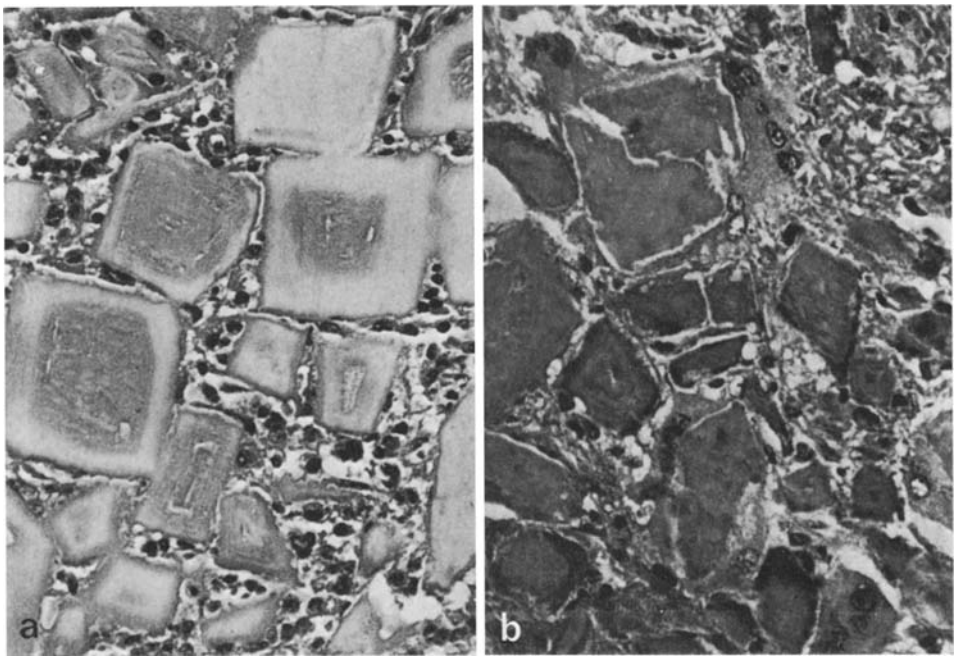


**Fig. 1.** Geometrically shaped deposits mixed with a plasma cell infiltrate (×160) **a.** Altered geometrically shaped structures surounded by multinucleated giant cells (×160) **b**

These crystalline structures are blue with Giemsa, faintly PAS positive, blue and pink with HPTM, red and green with Masson trichrome, salmon with Congo red, and highly fluorescent with thioflavine T. No birefringence is seen with Congo red. Some crystalline structures are slightly notched by argyrophilic fibres.

*Immunochemistry.* Immunoperoxidase studies demonstrate traces of IgG in crystalline structures and important positivity with lambda antisera in both cytoplasmic plasma cells and crystalline structures especially those located near plasma cell infiltration (Fig. 2a).

No IgM, IgA or K light chain are detected.

*Electron microscopy.* Ultrastructural study shows alterations of cells attributable to the biopsy procedure. However numerous, complete or fragmented crystalline structures, intermixed with cytoplasmic organelles are observed. These crystalline structures are made of several angular and concentric variable thickness coats of electron dense material (Fig. 2b). Sometimes, membrane units are seen at the interface of two coats. Nuclei distorted by crystalline structures without interposition of membrane units between them are also occasionally seen (Fig. 3a).

Myelomatous plasma cells are devoided of crystalline structures. They contain a large amount of rough endoplasmic reticulum.

Observations with optimised defocus at different magnifications (10,000

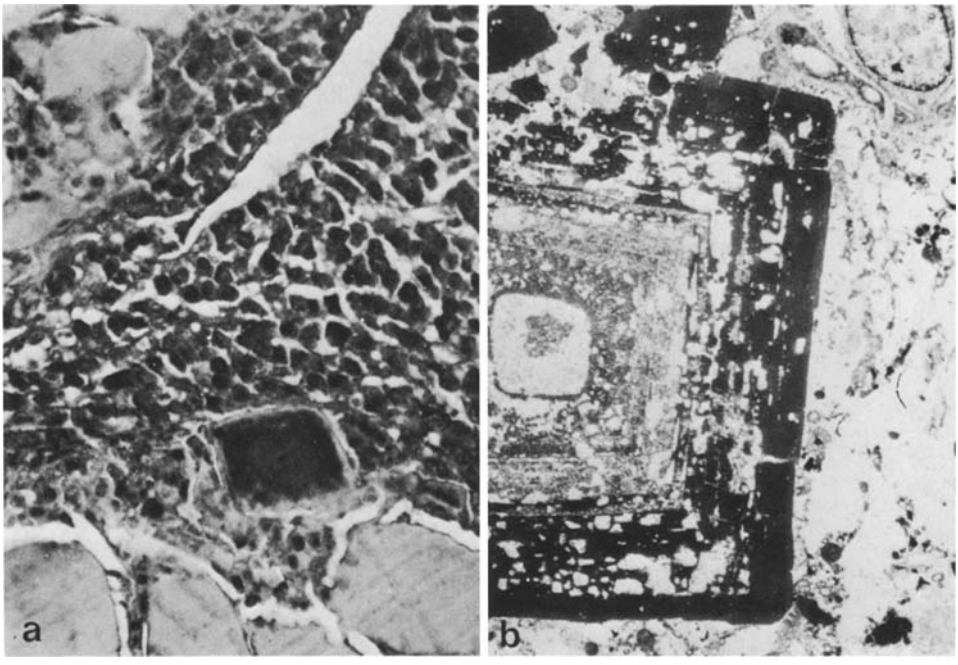


**Fig. 2a.** Immunohistochemical demonstration of lambda light chain in cytoplasm of plasma cells and crystalline structures (×160). **b.** Electron microscopy. Stratified crystalline structure (×2900)

to 200,000) of a great number of crystals with different stains and observations of unstained sections have never revealed ordered structure in images.

*Image analysis and processing.* When micrographs recorded in conditions described above are analysed by optical diffractometry, almost all diffractograms show spots of a typically periodic structure. The deduced values of periods vary with the orientation of the crystals. One to four lattice directions are identified, respective orientations of lattice change with crystals and lattices may disappear partially inside the same crystal.

Figure 3b shows some examples of optical diffractograms. The two mean measured spatial periods of the lattice are $5.6 \pm 0.6$ nm and $12 \pm 1$ nm. Processing images using filters shown in the left corner, point out clearly the different periodic structures (Fig. 3c, d) identified in diffractograms.

## Discussion

Cellular inclusions and deposits occur in association with many lymphoplasmacytic disorders, but these morphological features are not synonymous with malignancy.

In lymphoid cells, cytoplasmic or nuclear amorphous inclusions are observed in lymphoplasmacytic malignant lymphomas and multiple myelomas. They are also found in centrofollicular and immunoblastic malignant lym-

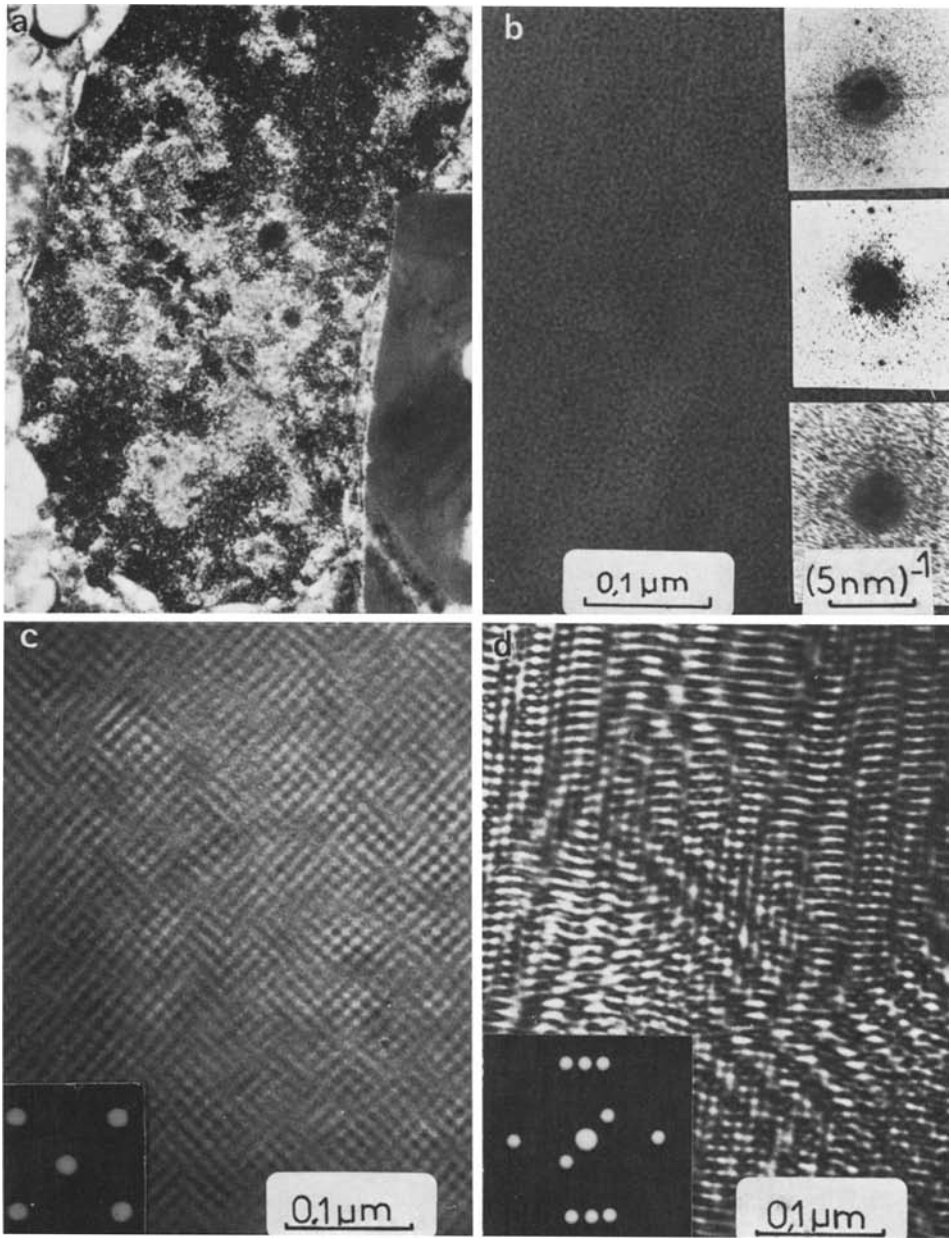


**Fig. 3a–d.** Electron microscopy and images processing. Nucleus notched by crystalline structure (×10500) **a.** Electron micrograph showing the amorphous look inside the "crystal" (×100000). Nevertheless (on the right side) optical diffraction of micrograph like this one points out periodic structures (about 5.5 and 11 nm) **b.** Analog processing (using filters shown in the left corner) of micrographs as **b** clearly shows reconstructed periodic structure images **c**, **d**

phomas and in inflammatory diseases and correspond to an accumulation of immunoglobulins in dilated ER and/or perinculear cisterna. They are the morphological expression of a deep disorder of synthesis and secretion of these proteins by lymphoid cells.

Interstitial amorphous deposits, localized or systemic, correspond to amyloid (Glenner 1980) and immunoglobulin deposits especially light chains (Randall et al. 1976). These features are generally consistent with plasma cell dyscrasias producing kappa or lambda light chain. Ultrastructural and immunohistochemical features help pathologists in the diagnosis of light chain deposits which fail to stain with thioflavine T and do not show birefringence with Congo red (Linder et al. 1983). Amyloid is the result of smaller polypeptide proteolysed light chain aggregating into a beta pleated sheet structure (Glenner 1980). Light chain deposits are the result of tissue deposits of aberrant size and secreted as polymer light chains (Preud'homme et al. 1980).

Crystalline cytoplasmic inclusions or interstitial deposits are uncommon in malignant lymphoplasmacytic disorders. Glaus (1917) first described myelomatous tumour nodules that contained rod like crystals in the ribs, vertebrae, sternum and long bones. More recently some observations of crystals in connective tissues (Brass 1943; Klintworth et. al 1978; Barr et al. 1980), in macrophages (Lennert 1978; Terashima et al. 1978), and in epithelial cells, especially of the proximal convoluted tubule (Sikl 1949; Ito et al. 1970; Mullen et al. 1981) with or without plasma cell inclusions, have been reported in multiple myeloma. Circulating kappa light chain, among the documented malignant cases, was associated with the deposits. Crystalline material of unknown origin, associated with asymptomatic M component have rarely been observed (Rodrigues et al. 1979; Eiferman et al. 1980). The size and shape of the crystals were varied. Ultrastructural periodicity and light chain antigen determinant detected by immunohistochemical methods were reported in some cases.

In this case the cristalline nature of the observed structures is indisputable. The geometric shape of these structures observed both in optical and electronic microscopy and the periodicities observed in the electron micrograph analysis agree with this conclusion. The periodicity of the lattices measured in all the crystals are $5.6 \pm 0.6$ nm and $12 \pm 1$ nm; the latter has already been seen in corneal crystal deposits (Rodrigues et al. 1979; Klinworth et al. 1978; Barr et al. 1980). Ito et al. have observed lattice structures of 6 to 9 nm periodicity in renal tubules from a patient with multiple myeloma. It is unlikely that the definite presence of occult periodicities arose from a fixation artifact. As far as we know periodic internal structure has never been identified in bone marrow crystal deposits from a patient with multiple myeloma.

Presence of IgG and lambda light chain in crystals located near plasma cells, suggest that crystals contain the whole or a fragmented constant portion of immunoglobulin as minor components. This observation is in agreement with Terashima's hypothesis (1978) that crystals are made in a large majority of a variable portion of immunoglobulin.

In this case membrane units observed between electron dense material coats allow us to conclude that crystals are either in the cytoplasm of macrophages or in the cytoplasm of plasma cells. However the particular layout of the coats which recall that of ER, is in our view an argument in favour of the latter, at least for the majority of crystals. Crystals in this case differ from Russel bodies according to their shape and size; furthermore Russel bodies show neither internal stratification nor smoth membrane units between coats (Ghadially 1975). Is is indeed possible that accumulated immunoglobulin in the cytoplasm of plasma cell are crystallised because of physicochemical variation. Dead cells would subsequently be ingested by macrophages. The particular localisation of crystals at the center of bone marrow spaces favours our hypothesis.

*Acknowledgments.* The skillful help of E. Martin, B. Liger, M. Vauchelin, M. Lhotel and G. Boude is greatly acknowledged.

## References

Barr CC, Gelender H, Font RL (1980) Corneal crystalline deposits associated with dysproteinemia. Arch Ophtalmol 98:884–889

Brass K (1943) Die Einweisstoffwechseltonungen des Plasmocytomkranken. Frankfurt 2 Pathol 57:367–380

Eiferman RA, Rodrigues MM (1980) Unusual superficial stroma corneal deposits in IgGK monoclonal gammopathy. Arch Ophtalmol 98:78–81

Ghadially FN (1975) Ultrastructural pathology of the cell. Butterworths (ed) 244–246

Glaus A (1917) Über multiples Myelozytoma mit eigenartigen, zum Teil Krystallähnlichen Zelleneinlagerungen, Kombiniert mit Elastose und ausgedehnter Amyloidose und Verkalkung. Virchows Arch [Pathol Anat] 223:301–339

Glenner GG (1980) Amyloid deposits and amyloidosis. The B-fibrilloses. N Engl J Med 302:1283–1292, 1333–1343

Hanszen KJ (1971) The optical transfer theory of the electron microscopy: fundamental principes and applications, in: Barer R, Cosslett VE (eds) Advances in optical and electron microscopy. Academic Press, London, New York

Harburun G, Ranniko JK (1972) An Improved optical diffractometer. J Phys E (Sci Instr) 5:757–762

Ito S, Goshima K, Ninomi M, Horikoshi N, Nomura S, Sugiora K, Yamazaki K, Hirabayashi N, Nishi Y (1970) Electron microscopic studies of crystalline inclusions in the myeloma cells and kidneys of K-Bence-Jones protein type myeloma. Acta Haemat Jpn 33:598–617

Jeannette JC, Wilman AS, Benson JD (1981) IgD myeloma with intracytoplasmic crystallin inclusions. Amer J Clin Pathol 75:231–235

Klintworth GK, Bredehoeft SJ, Reed JW (1978) Analysis of corneal crystalline deposits in multiple myeloma. Am J Ophtalmol 86:303–313

Klug A, Berger JE (1964) An optical method for the analysis of periodicities in electron micrographs, and some observations on the mechanism of negative staining. Journal of Molecular Biology, 10:565–569

Klug A, de Rosier DJ (1966) Optical filtering of electron micrographs: reconstruction of one-sided images. Nature 212:29–32

Lennert K (1978) Malignant lymphomas other than Hodkin's disease. Springer, Berlin Heidelberg New York 260

Linder J, Vollmer RT, Groker BP, Shelburne J (1983) Systemic kappa light chain deposition. An ultrastructural and immunohistochemical study. Am J Surg Pathol 7:85–93

Mullen B, Chalvardjan A (1981) Crystalline tissue deposits in a case of multiple myeloma. Arch Pathol Lab Med 105:94–97

Preud'homme JL, Morel-Maroger L, Brouet JC, Cerf M, Mignon F, Gugliemi P, Seligmann

M (1980) Synthesis of abnormal immunoglobulins in lymphoplasmocytic disorders with visceral light chain deposition. Am J Med 69:703–710
Randall RE, Williamson WC, Mullinax F, Tung MY, Still WJS (1976) Manifestations of systemic light chain deposition. Am J Med 60:293–299
Rodriguez MM, Krachmer JH, Miller SD, Newsome DA (1979) Posterior corneal crystalline deposits in benign monoclonal gammopathy. Arch Ophtalmol 97:124–128
Sikl H (1949) A case of diffuse plasmocytosis with deposition of protein crystals in the kidney. J Pathol Bacteriol 61:149–163
Terashima K, Takahashi K, Kojima M, Imai Y, Tsuchida S, Migita S, Ebina S, Itoh C (1978) Kappa-type light chain crystal storage histiocytosis. Acta Path Jpn 28 (1):11–138

Accepted June 4, 1985